

## Magnetic nano-grains from a non-magnetic material: a possible explanation

Endre Kovács<sup>1</sup>, Réka Trencsényi<sup>2</sup>, and Zsolt Gulácsi<sup>2</sup>

<sup>1</sup> Department of Physics, University of Miskolc, Miskolc, Hungary

<sup>2</sup> Department of Theoretical Physics, University of Debrecen, Debrecen, Hungary

E-mail: [fizendre@uni-miskolc.hu](mailto:fizendre@uni-miskolc.hu)

**Abstract.** Based on positive semidefinite operator properties, an exact ground state solution is deduced for a 2D Hubbard model with periodic boundary conditions on small samples. The obtained ferromagnetic behavior is used as a possible explanation of the ferromagnetism occurring in nano-samples made of non-magnetic but metallic materials.

### 1. Introduction

It is known that if a sample is constructed from non-magnetic metal (for example Au), and the size of the object is decreased to nanoscale values, the material can become ferromagnetic [1,2]. Below we provide a possible explanation for this effect, which requires only Coulomb repulsion between itinerant carriers, closed surface and quantum mechanical effects. For this reason we analyze a two dimensional  $L \times L$  square lattice at arbitrary but finite  $L$  size with periodic boundary conditions in both directions, containing itinerant electrons. The Coulomb repulsion in this many-body system is screened by the itinerant system, consequently is of short-range type, and hence is taken into account for simplicity by the on-site Coulomb repulsion alone. Below this Hubbard system is solved exactly for the ground state in a restricted region of the parameter space, obtaining a ferromagnetic solution for small  $L$  values.

The solution procedure (see [3-7] for details) is based on positive semidefinite operator properties. The technique first transforms in exact terms the Hamiltonian  $\hat{H}$  of the system in a positive semidefinite form  $\hat{H} = \hat{P} + C$  where  $\hat{P}$  is a positive semidefinite operator while  $C$  is a constant scalar. Since the spectrum of  $\hat{P}$  is bounded from below by the zero minimum eigenvalue, in the second step one deduces the exact ground state  $|\Psi_g\rangle$  by constructing the most general wave vector which satisfies the relation  $\hat{P}|\Psi_g\rangle = 0$ . The ground state energy becomes  $E_g = C$ . The ground state turns out to be ferromagnetic if the number of electrons  $N \in (L, 2L)$  and has the form  $|\Psi_g\rangle = \prod_i \hat{B}_{i,\sigma}^\dagger |0\rangle$  where  $|0\rangle$  represents the bare vacuum state, and  $\hat{B}_{i,\sigma}^\dagger$  are operators which extend along the whole system holding a specific vortex structure, being built up from linear combinations of creation Fermi operators with fixed spin projection  $\sigma$  acting on different sites of the lattice. The parameter space region where the solution emerges is not severely restricted, and flat bands in the bare band structure are not present.

The periodic boundary conditions in two dimensions and both directions lead to a closed surface which reproduces a metallic grain, which, because of the Coulomb repulsion between



the carriers, holds mobile electrons only on its surface.  $\hat{H}$  has only on-site interaction terms and fixed hopping matrix elements, hence is not sensitive to folding and not requires a specific shape of the closed surface. If the grain is macroscopic ( $L \sim 10^{26}$ ), the concentration range ( $\rho = L/L^2 \sim 1/L$ ) where the effect emerges  $\rho = 10^{-26} \sim 0$  is practically missing. But for nanoscale, for example  $L=10$ , leading to  $\rho = 1/10$ , the effect is observable, and the nano-grain behaves as a ferromagnetic object.

The remaining part of the paper presents the details of the calculation as follows: Sect. 2. describes the used Hamiltonian, Sect. 3. shows how the transformation of  $\hat{H}$  in positive semidefinite form is made, Sect. 4. presents the deduced ground state, and finally Sect. 5. containing the summary closes the presentation.

## 2. The Hamiltonian

We consider the Hubbard model on a 2D Bravais lattice with primitive vectors

$\mathbf{x}, \mathbf{y}$  and  $N_\Lambda = L \times L$  lattice sites given by  $\hat{H} = \hat{H}_0 + \hat{H}_U$ , where

$$\begin{aligned} \hat{H}_0 &= \sum_{\mathbf{i}, \sigma} (t_x \hat{c}_{\mathbf{i}+\mathbf{x}, \sigma}^\dagger \hat{c}_{\mathbf{i}, \sigma} + t_y \hat{c}_{\mathbf{i}+\mathbf{y}, \sigma}^\dagger \hat{c}_{\mathbf{i}, \sigma} + t_{y+\mathbf{x}} \hat{c}_{\mathbf{i}+\mathbf{x}+\mathbf{y}, \sigma}^\dagger \hat{c}_{\mathbf{i}, \sigma} + t_{y-\mathbf{x}} \hat{c}_{\mathbf{i}+\mathbf{y}-\mathbf{x}, \sigma}^\dagger \hat{c}_{\mathbf{i}, \sigma} + H.c.) \\ \hat{H}_U &= U \sum_{\mathbf{i}} \hat{n}_{\mathbf{i}, \uparrow} \hat{n}_{\mathbf{i}, \downarrow}, \quad U > 0. \end{aligned} \quad (1)$$

Here  $t_x, (t_y)$  are the nearest neighbor hopping amplitudes along the bonds in the  $\mathbf{x}, (\mathbf{y})$  direction, and  $t_{y+\mathbf{x}}, (t_{y-\mathbf{x}})$  are the next nearest neighbor hoppings taken along cell diagonals in  $\mathbf{y} + \mathbf{x}, (\mathbf{y} - \mathbf{x})$  directions, while  $\hat{H}_U$  represents the Hubbard interaction.

Using the  $\hat{c}_{\mathbf{i}, \sigma} = (1/\sqrt{N_\Lambda}) \sum_{\mathbf{k}} e^{-i\mathbf{k}\mathbf{i}} \hat{c}_{\mathbf{k}, \sigma}$  expressions for the Fourier transforms, the kinetic part  $\hat{H}_0$  has the  $\mathbf{k}$ -space form

$$\begin{aligned} \hat{H}_0 &= \sum_{\mathbf{k}, \sigma} [(t_x e^{+i\mathbf{k}\mathbf{x}} + t_x^* e^{-i\mathbf{k}\mathbf{x}}) + (t_y e^{+i\mathbf{k}\mathbf{y}} + t_y^* e^{-i\mathbf{k}\mathbf{y}}) + (t_{y+\mathbf{x}} e^{+i\mathbf{k}(\mathbf{y}+\mathbf{x})} + t_{y+\mathbf{x}}^* e^{-i\mathbf{k}(\mathbf{y}+\mathbf{x})}) \\ &\quad + (t_{y-\mathbf{x}} e^{+i\mathbf{k}(\mathbf{y}-\mathbf{x})} + t_{y-\mathbf{x}}^* e^{-i\mathbf{k}(\mathbf{y}-\mathbf{x})})] \hat{c}_{\mathbf{k}, \sigma}^\dagger \hat{c}_{\mathbf{k}, \sigma}. \end{aligned} \quad (2)$$

For the simplest symmetric case  $t_1 \doteq t_x = t_y$ ,  $t_2 \doteq t_{y+\mathbf{x}} = t_{y-\mathbf{x}}$ , we obtain the following dispersion relation:

$$\epsilon_{\mathbf{k}} = 2t_1 (\cos k_x + \cos k_y) + 4t_2 \cos k_x \cos k_y, \quad (3)$$

which, except for the trivial case  $t_1 = t_2 = 0$ , cannot be made flat.

## 3. The positive semidefinite transformation of the Hamiltonian

Let us consider on each site  $\mathbf{i}$  of the lattice the block operator (or cell operator) defined on the cell constructed on the site  $\mathbf{i}$  containing the sites  $(\mathbf{i}, \mathbf{i} + \mathbf{x}, \mathbf{i} + \mathbf{x} + \mathbf{y}, \mathbf{i} + \mathbf{y})$ :

$$\hat{A}_{\mathbf{i}, \sigma} = a_1 \hat{c}_{\mathbf{i}, \sigma} + a_2 \hat{c}_{\mathbf{i}+\mathbf{x}, \sigma} + a_3 \hat{c}_{\mathbf{i}+\mathbf{x}+\mathbf{y}, \sigma} + a_4 \hat{c}_{\mathbf{i}+\mathbf{y}, \sigma}, \quad (4)$$

where the  $a_n$  coefficients are defined at the site denoted by  $n$  inside the cell (see Fig.1).

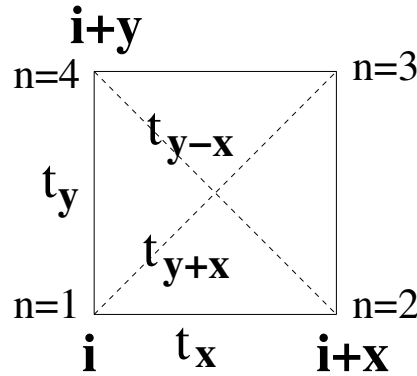


Fig. 1: The notations used in defining the  $\hat{A}_{i,\sigma}$  operator: The presented cell is defined at the site  $\mathbf{i}$ , the  $\mathbf{x}$ ,  $\mathbf{y}$  are the primitive vectors of the lattice,  $n$  denotes the sites inside the cell,  $t_x, t_y$  are the hopping matrix elements connecting nearest-neighbor sites, while the next nearest-neighbor hoppings  $t_{y+x}$  and  $t_{y-x}$  are present along diagonals plotted by the dashed lines.

We note that since  $U > 0$ , the Hubbard term is automatically positive semidefinite. Now the Hamiltonian from (1) becomes

$$\hat{H} = \hat{P} - K\hat{N} = \sum_{i,\sigma} \hat{A}_{i,\sigma}^\dagger \hat{A}_{i,\sigma} + \hat{H}_U - K\hat{N} \quad (5)$$

if the following matching conditions are satisfied:

$$\begin{aligned} t_x &= a_2^* a_1 + a_3^* a_4, & t_{y+x} &= a_3^* a_1, \\ t_y &= a_4^* a_1 + a_3^* a_2, & t_{y-x} &= a_4^* a_2. \end{aligned} \quad (6)$$

Besides, the  $K$  coefficient in (6) is given by

$$K = |a_1|^2 + |a_2|^2 + |a_3|^2 + |a_4|^2. \quad (7)$$

We have found several different solutions of this system of complex nonlinear equations. Here we present only the simplest one, the symmetric isotropic case.

$$\begin{aligned} t_1 &\doteq t_x = t_y = 2|a_1|^2, \\ t_2 &\doteq t_{y+x} = t_{y-x} = |a_1|^2, \end{aligned}$$

where the conditions  $t_i > 0$  ( $i \in \{x, y, y+x, y-x\}$ ) and  $t_2 = t_1/2$  must hold. One can see that these conditions are not at all unrealistic and not too restrictive. The ground state energy is  $E_g = -4t_1 N$ .

#### 4. The ground state

Now we analyze the Hamiltonian (5), and look for a ground state of the form

$$|\Psi_g\rangle = \prod_i \hat{D}_{i,\sigma_i}^\dagger |0\rangle. \quad (8)$$

If such a state exists, in order to provide  $\sum_{i,\sigma} \hat{A}_{i,\sigma}^\dagger \hat{A}_{i,\sigma} |\Psi_g\rangle = 0$  (e.g. to be in the kernel of the first term of  $\hat{H}$ ), the  $\hat{A}_{i,\sigma}$  operator must satisfy

$$\{\hat{A}_{i,\sigma}, \hat{D}_{j,\sigma_j}^\dagger\} = 0 \quad (9)$$

for all values of all indices. Furthermore, the wave function (8) is in the kernel of  $\hat{H}_U$  if there are no doubly occupied sites in the system. Now we try to deduce the possible expression of the  $\hat{D}_{j,\sigma_j}^\dagger$  operator.

Starting the deduction of the  $\hat{D}_{j,\sigma_j}^\dagger$  operator, one must pay attention to the following aspect: Being only one type of fermionic operator present in  $\hat{H}$ , namely  $\hat{c}_{i,\sigma}$ , in order to obtain a  $\hat{D}_{j,\sigma_j}^\dagger$  satisfying (9), all operators  $\hat{A}_{i,\sigma}$  must share with  $\hat{D}_{j,\sigma_j}^\dagger$  zero, or at least two lattice sites. The main information here is that for all indices, the  $\hat{A}_{i,\sigma}$  operator must not touch  $\hat{D}_{j,\sigma_j}^\dagger$  in a single point. This is possible only if  $\hat{D}_{j,\sigma_j}^\dagger$  is extended along the whole system.

To satisfy this condition, let us consider a general expression for the  $\hat{D}_{j,\sigma_j}^\dagger$  operator collecting additive contributions from all lattice sites of the system. The mathematical expression of the  $\hat{D}_{j,\sigma_j}^\dagger$  operator then becomes

$$\hat{D}_{j,\sigma_j}^\dagger = \sum_{i=1}^L \sum_{j=1}^L x_{i,j} \hat{c}_{(i-1)\mathbf{x}+(j-1)\mathbf{y},\sigma}^\dagger, \quad (10)$$

where  $\mathbf{x}, \mathbf{y}$  are the primitive vectors, and in the  $x_{i,j}$  coefficients the  $i$  is the row index, while  $j$  is the column index.

Since in (9) one can have  $L^2$  different  $\hat{A}_{i,\sigma}$  operators for a fixed  $\sigma$  spin projection, in order to deduce the  $x_{i,j}$  coefficients from (9), one obtains  $2L^2$  different equations. The first one for example is the following:

$$a_1 x_{1,1} + a_2 x_{1,2} + a_3 x_{n,2} + a_4 x_{n,1} = 0$$

Usually the solutions can be deduced for finite  $L$ , and the obtained result must be extended to arbitrary large  $L$ . We show in a simple symmetric and isotropic case that this can be performed, indeed.

One  $\hat{D}^\dagger$  operator obtained for this case at  $L=12$  is presented in Fig. 2. As one can see from this figure, the displacement of particles inside  $\hat{D}_{j,\sigma_j}^\dagger$  follows vortex lines. These lines are displaced around 4 equivalent vortex centers (denoted by dotted squares in the figure) whose position can serve in denoting different  $\hat{D}_{j,\sigma_j}^\dagger$  operators. For example the bottom-left site of a vortex center can serve for the  $\mathbf{j}$  index of the operator  $\hat{D}_{j,\sigma_j}^\dagger$ . The spin index  $\sigma_j$  of the operator  $\hat{D}_{j,\sigma_j}^\dagger$  is the same on all sites. Modifying the position of the vortex center, one finds new  $\hat{D}^\dagger$  operators.

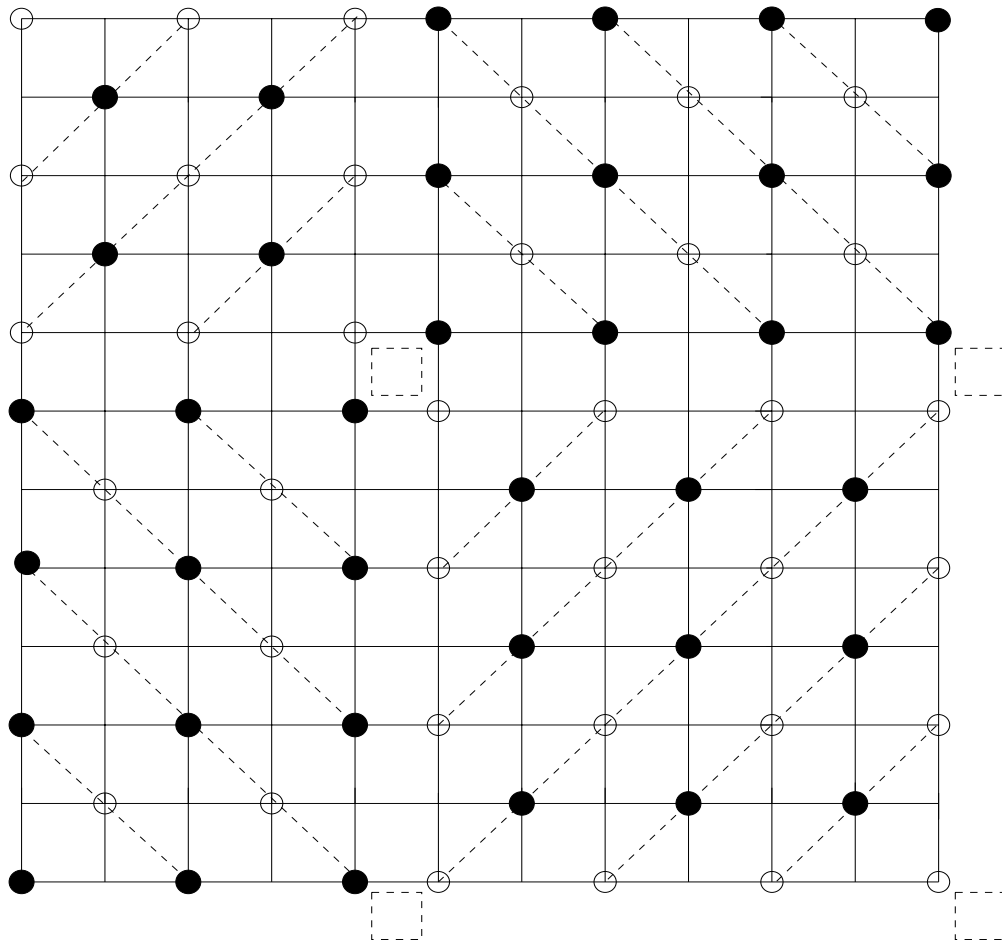


Fig.2. A  $\hat{D}_{j,\sigma_j}^\dagger$  operator deduced at  $L=12$ . Black dots at an arbitrary site  $\mathbf{i}$  are representing  $-\hat{c}_{\mathbf{i},\sigma}^\dagger$ , and white dots at a site  $\mathbf{i}$  are representing  $+\hat{c}_{\mathbf{i},\sigma}^\dagger$  operators. All these contributions presented in the figure must be added providing the deduced  $\hat{D}_{j,\sigma_j}^\dagger$ . The dotted lines represent a guide for the eyes. The dotted squares are representing 4 equivalent plaquettes in the construction of  $\hat{D}_{j,\sigma_j}^\dagger$ . It can be seen that the extension of the solution to an arbitrary large system (for even  $L$ ) is possible.

In obtaining the mathematical expression of the  $\hat{D}_{j,\sigma_j}^\dagger$  operator from Fig.2., one takes into consideration that black dots placed at an arbitrary site  $\mathbf{i}$  are representing  $-\hat{c}_{\mathbf{i},\sigma}^\dagger$  operators, while white dots at an arbitrary site  $\mathbf{i}$  are representing  $+\hat{c}_{\mathbf{i},\sigma}^\dagger$  operators. Adding all contributions from Fig.2 one obtains the mathematical expression of the plotted  $\hat{D}^\dagger$  operator. Fig.2 shows that the  $\hat{D}^\dagger$  solution obtained for a  $12 \times 12$  lattice can be generalized to an arbitrary large system (for even  $L$ ).

Different linearly independent  $\hat{D}^\dagger$  operators can be obtained by modifying the position of the vortex center. Since for all (even)  $L$ , four equivalent vortex center positions exist, at first

view it seems that  $N_\Lambda / 4$  linearly independent  $\hat{D}^\dagger$  operators exist. However, if we directly check the linear independence, it turns out that only  $L$  of them are linearly independent.

The product of all linearly independent  $\hat{D}^\dagger$  operators leads to touching points between all components of the product. To enter also in the kernel of  $\hat{H}_U$ , the spin index for all  $\hat{D}_{j,\sigma_j}^\dagger$  operators will be fixed to the same value  $\sigma_j = \sigma$ , hence the ground state becomes

$$|\Psi_g\rangle = \prod_j \hat{D}_{j,\sigma}^\dagger |0\rangle, \quad (11)$$

which represents a saturated ferromagnetic state.

## 5. Summary

By applying a technique based on the properties of positive semidefinite operators we analyzed a two dimensional system with periodic boundary conditions, where the Hubbard on-site Coulomb repulsion acts between the itinerant electrons. For small samples ferromagnetism has been found which disappears when the size of the system increases. The results provide a possible explanation for the emergence of ferromagnetism on metallic nano-grains built up from a non-magnetic material. The deduced result does not require rigorous spherical surface, nor spin-orbit interaction: it demands only itinerant electrons on a closed surface, Coulomb repulsion between the carriers, and quantum mechanic many-body behavior.

## ACKNOWLEDGEMENTS

We kindly acknowledge financial support of the following contracts: for E.K. TAMOP-4.2.1.B-10/2/KONV-2010-0001, for R.T. TAMOP-4.2.2/B-10/1-2010-0024 and for Z.G. OTKA-K-100288, TAMOP-4.2.1/B-09/1/KONV-2010-0007, and Alexander von Humboldt Foundation.

## References

- [1] P. Crespo, R. Litran, T. C. Rojas, et al. Phys. Rev. Lett. **93**, 087204 (2004)
- [2] S. Banerjee, S. O. Raja, M. Sardar et al. Cond-mat arXiv:0912.3319
- [3] Z. Gulacsi, A. Kampf, D. Vollhardt, Phys. Rev. Lett. **105**, 266403 (2010);
- [4] Z. Gulacsi, D. Vollhardt, Phys. Rev. Lett. **91**, 186401 (2003)
- [5] Z. Gulácsi, A. Kampf, D. Vollhardt, Phys. Rev. Lett. **99**, 026404 (2007).
- [6] R. Trencsenyi, K. Gulacsi, E. Kovacs, Z. Gulacsi, Ann. der Phys (Berlin) **523**, 741 (2011).
- [7] R. Trencsényi, E. Kovács, Z. Gulácsi, Phil. Mag. B, **89**, 1953 (2009).